

Fractal Stability Border in Plane Couette Flow

Armin Schmiegel and Bruno Eckhardt

*Fachbereich Physik und Institut für Chemie und Biologie des Meeres,
der C.v. Ossietzky Universität, Postfach 25 03, D-26111 Oldenburg, Germany*

and

*Fachbereich Physik der Philipps Universität Marburg, D-35032 Marburg, Germany
(permanent)*

(October 31, 2018)

We study the dynamics of localised perturbations in plane Couette flow with periodic lateral boundary conditions. For small Reynolds number and small amplitude of the initial state the perturbation decays on a viscous time scale $t \propto Re$. For Reynolds number larger than about 200, chaotic transients appear with life times longer than the viscous one. Depending on the type of the perturbation isolated initial conditions with infinite life time appear for Reynolds numbers larger than about 270–320. In this third regime, the life time as a function of Reynolds number and amplitude is fractal. These results suggest that in the transition region the turbulent dynamics is characterised by a chaotic repeller rather than an attractor.

47.20.Ft,47.20.Ky,47.15.Fe,05.45.+b

For a variety of simple flows linear stability theory predicts and experiments verify that the transition to turbulence proceeds by a sequence of instabilities at well defined critical values of the control parameter [1,2]. Prominent examples include a layer of fluid heated from below, flow between rotating cylinders, liquid jets, and stratified fluids. The transition to turbulence in pipe flow [3] or plane Couette flow [4,5] and to spiral turbulence in the flow between counter-rotating cylinders [6] does not fit this pattern. If the Reynolds number is sufficiently large, turbulent dynamics can occur although the laminar profile is still stable. A formal linear stability analysis predicts either no instability (as in plane Couette flow [7]) or one for Reynolds numbers larger than the ones where experiments begin to show turbulent behavior (e.g. plane Poiseuille flow [8]). The nature of the transition is different from the cases with a linear instability. It depends on the size of the perturbation [9], shows very strong intermittency [10,11] and has no sharply defined stability border [3].

Such observations can be explained, if the bifurcations are sub critical, for then the new state extends to lower values of the Reynolds number and can be reached starting from finite amplitude perturbations [12–14]. Simple models, based on interacting wave vector triads or truncations of Galerkin systems, are compatible with this view. However, it has not been possible to follow these upper branches all the way down to where they (dis-)appear and to identify a critical Reynolds number.

A different approach has recently focused on the eigenvectors of the linearised problem [15–18]. Very often the linearised hydrodynamic eigenvalue problem is not hermitian, so that the eigenvectors are not orthogonal. As a consequence, even for (negative) eigenvalues, small perturbations can be amplified a lot, so that the neglect of nonlinear interactions no longer can be justified. This explains how in the absence of linear instability the stability region around the laminar profile becomes small, perhaps

irrelevantly small. One can imagine that because of this growth some of the turbulence seen in these systems is noise induced [18].

To shed some more light on the dynamics in these cases, we have studied the evolution of perturbations in a numerical model for plane Couette flow. The numerical method was designed specifically to allow accurate long integration times. The life time of these perturbations was mapped out in an amplitude-Reynolds number plane. This allowed to identify three dynamical regimes and to study the transitions between them. The results indicate that there is no sharp transition to turbulence: the landscape of life times has fractal features, with some isolated life times longer than the finite integration time. Thus, whether an initial condition leads to an evolution identified as turbulent depends in a sensitive way on initial amplitude, Reynolds number and the experimental observation time. This is in qualitative agreement with experiments on plane Couette flow [4,5] and consistent with observations on pipe flow [3]. In addition, the numerical results suggest that the turbulent state belongs to a transient repeller rather than a turbulent attractor [19,20].

The numerical model (see [21] for more details) is based on an expansion of the velocity field in Fourier and Legendre polynomials,

$$\mathbf{u}(x, y, z, t) = \sum_{\mathbf{k}, p} \tilde{\mathbf{u}}_{\mathbf{k}, p}(t) e^{i(k_x x + k_y y)} L_p(z). \quad (1)$$

The advantage of Legendre polynomials compared to Chebyshev polynomials is that they give rise to evolution equations which are energy conserving in the Eulerian, undriven limit. This is important for the long time evolution we want to study. For every velocity-component, we used a set of 37 Fourier modes on a hexagonal grid and 16 Legendre-polynomials. The boundary conditions $\mathbf{u}(x, z, \pm H/2) = 0$ and continuity equation are included within the Lagrange formalism of the first kind

[21]. These restrictions finally leave 962 dynamically active degrees of freedom.

The basic flow is normalised to have velocity $\pm U_0$ at $z = \pm H/2$. The Reynolds number is defined as $Re = U_0 H/2\nu$, with ν the kinematic viscosity. Lengths are measured in units of $H/2$ and time in units of $\tau = H/2U_0$. The Navier-Stokes equation for a perturbation \mathbf{u} of the initial profile $\mathbf{U}_0 = U_0 z \mathbf{e}_x$,

$$\dot{\mathbf{u}} = -(\mathbf{u} \cdot \nabla) \mathbf{U}_0 + (\mathbf{U}_0 \cdot \nabla) \mathbf{u} - (\mathbf{u} \cdot \nabla) \mathbf{u} - \frac{1}{\rho} \nabla p + \frac{1}{Re} \Delta \mathbf{u} \quad (2)$$

$$\nabla \mathbf{u} = 0, \quad (3)$$

are replaced by nonlinear ordinary differential equations for the amplitudes $\hat{\mathbf{u}}_{\mathbf{k},p}$. It was verified that the time evolution could be followed sufficiently accurately for scaled times up to 10000. For $h = 1 \text{ cm}$, the viscosity of water and a Reynolds number of $Re = 400$ this corresponds to about 9 min . In experiments a localised initial disturbance spreads and reaches the span wise walls within less than a minute [22,23]. The numerical calculations thus extend to a time region where in experiments the influence of the lateral walls are no longer negligible.

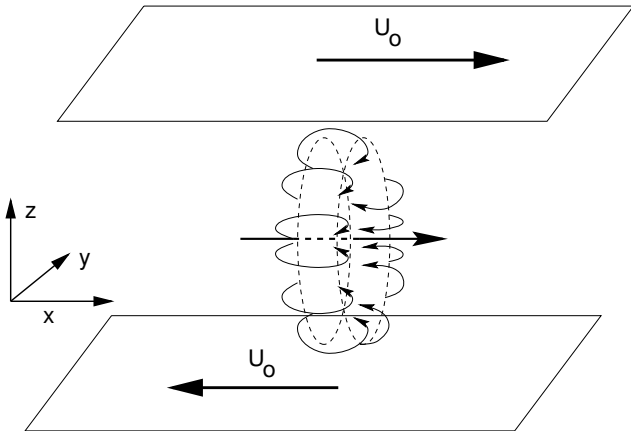


FIG. 1. Sketch of the poloidal vortex-ring (4) used as initial condition.

The initial state for our simulations was taken to be a poloidal vortex ring in the y -, z -plane,

$$\mathbf{u} = A \text{curl curl} \delta(x, y) e^{-10z^2} \mathbf{e}_x, \quad (4)$$

with a variable amplitude A . We approximate the δ function by setting all real Fourier modes equal to one. As shown schematically in Fig. 1, the axis of the ring points in the \mathbf{e}_x -direction. To remove excess energy for large modes we integrated this state for five time units at $Re = 400$ and used the resulting physically realistic initial condition in the subsequent studies. By this time the vortex ring has been rotated into the x -, y -plane and is similar to the one induced by the vertical water jets in the experiments of Bergé et al. [4,22,24].

Three different flow regimes are distinguishable by their time series as shown in Fig. 2. For low Reynolds number, the energy of the perturbation decays smoothly, with a bump related to the non-normality of the linearised equations of motion. The time when this maximum is reached is in agreement with the estimate $t_{max} \propto 0.117 Re$ in [25]. This is the first regime, dominated by the linearised equations.

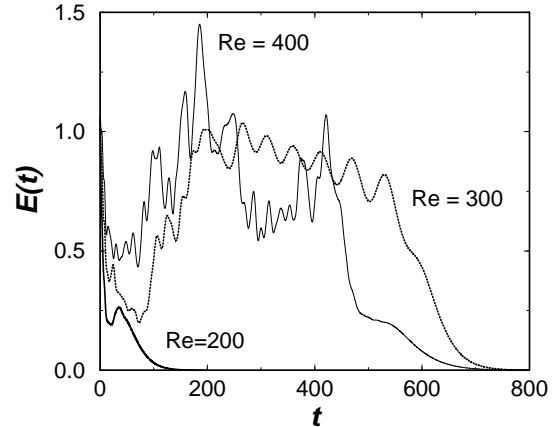


FIG. 2. Evolution of the energy in the perturbation *vs.* time for three values of the Reynolds number.

Around $Re = 300$ states show a qualitatively similar decay but only after an intermediate period of irregular dynamics. A life time can be defined by monitoring the z -component of the velocity until it decays below a certain threshold. If that happens the perturbation lacks the driving and decays as described by the linearised equations. In this second flow regime the life times for perturbations are longer than estimated from the linearised equations. But one notes from Fig. 2 that the life time of the disturbance is not a monotonic function of Re : The evolution at $Re = 400$ shows more fluctuations and violent bursts but its life time is shorter than at $Re = 300$. In this third region, characterised by a non-monotonous variation of life times with amplitude and Reynolds number, some initial conditions do not decay within the numerical integration time. The signal for the decaying and non-decaying states are dynamically similar in the fluctuating states, and there is no precursor that indicates the decay of the perturbation.

The non-monotonous variations of life time with Reynolds number and amplitude occur for Re above about 350 and cover an increasing range in amplitude. On a global scale (Fig. 3), one notes a rather ragged landscape with a few peaks reaching up to the maximal life times followed in the numerical calculations. Because of the finite observation times in experiments states are classified as decaying or turbulent according to the life times being above or below a certain threshold. Such a cut through the life time landscape shows isolated turbulent disturbances in the decaying region and isolated

decaying disturbances in the turbulent region. Such behavior has been seen in experiments on constant mass flow through a pipe [3]. The non-monotonicity observed there may thus be of dynamical origin and not due to experimental limitations.

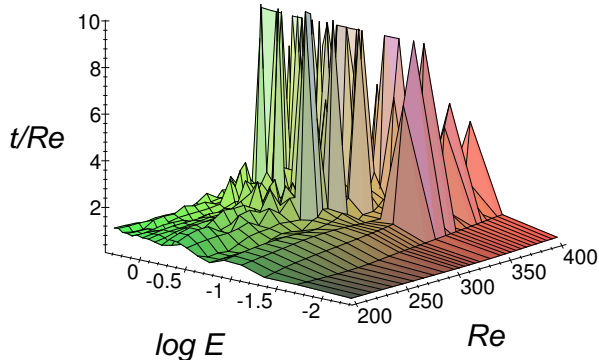


FIG. 3. Lifetime *vs* Reynolds number *Re* and energy of the initial state. The life time is normalised by *Re*, so that in the linear viscous regime for small *Re* one expects a constant. Integration was stopped after a scaled time of 3000 units.

The distribution of life times as a function of amplitude and Reynolds number has fractal features. Magnification of successive intervals in amplitude (Fig. 4) for fixed Reynolds number or of intervals in *Re* for fixed amplitude reveals a self similar pattern of life times, without any obvious simplifications on smaller scales. The magnifications are reminiscent of life time pictures obtained in chaotic scattering [26–28]. This analogy suggests that the long life times arise for initial perturbations which are close to the stable manifold of saddles in phase space. Then arbitrarily large life times should be possible and the ‘turbulent’ state would be supported by a repeller rather than an attractor.

The magnifications in Fig. 4 give no indication that the peaks with large life times have a finite width, in accord with the repeller picture. The sensitivity of the life time to the initial state can be quantified in terms of the uncertainty dimension [28]. For a given uncertainty in the amplitude ϵ , we calculate the probability $f(\epsilon)$ to find disturbance with life times greater than a given limit $t_{\max} = 3000$. For fractal sets, this probability decreases with decreasing ϵ , with a scaling exponent α , $f(\epsilon) \propto \epsilon^\alpha$. The uncertainty dimension is then given by $d_s = 1 - \alpha$. For $Re = 400$ we find a scaling exponent $\alpha \approx 0.29$ and an uncertainty dimension $d_s \approx 0.71$.

As the Reynolds number increases the number of long lived disturbances increases and they cover an ever increasing region in phase space and extend to smaller amplitudes. Phase space becomes more densely filled with

the stable and unstable manifolds of the saddles so that trajectories trapped in this tangle need more and more time before they can escape and relax to the laminar profile. This is in line with previous observations in large systems [19] and pipe flow [29] that long lived transients can imitate a permanent turbulent state. Clearly a measure of the thickness of the repeller or an estimate of the life time of transients as a function of Reynolds number would be highly desirable but is presently beyond our numerical or analytical abilities.

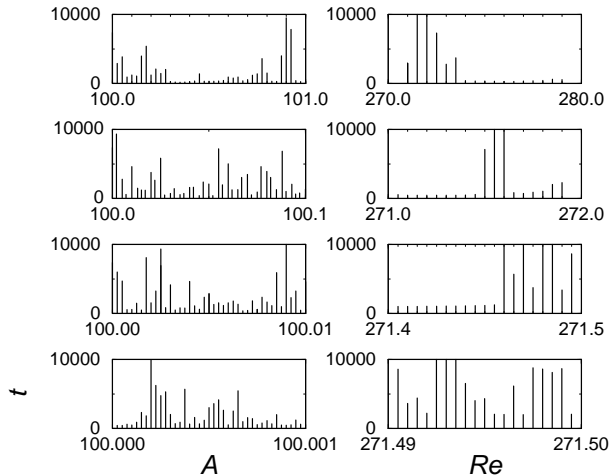


FIG. 4. Successive magnifications of cuts through the life-time landscape of Fig. 3, for $Re = 400$ and varying amplitude (left column) and for fixed amplitude $A = 100$ and varying Reynolds number (right column).

Further support for these observations is derived from a low dimensional system of ordinary differential equations for a shear flow where we can follow the dynamics more efficiently and can also study the nature of the repeller in more detail [30]. In particular, we find that the repeller is built around a rapidly increasing number of stationary states which are born in saddle-node bifurcations above a critical Reynolds number. All states are unstable and the dimension of the repeller is rather high-dimensional. In the present flow the time intervals on the repeller are too short and the dimensions presumably too high to allow for a determination of its fractal dimension. An indication of its dimension is given by the number of unstable eigenvalues of the local linearization. In our simulation of plane Couette flow at $Re = 400$ this number lies between 30 and 80 positive eigenvalues. The maximum eigenvalue of the local linearization was about 0.35 in inverse time units.

Candidates for repeller states in plane Couette flow are the stationary states found by Nagata [31] and Clever and Busse [32,33]. These states appear for Reynolds numbers above about 125. For larger Reynolds numbers we have

found further states, in accord with the observations on the model. But there remains a discrepancy between the Reynolds number for the occurrence of stationary states (about 125) and the one where the dynamics shows turbulence. However, the latter depends strongly on the initial conditions. For the ones presented above, the long lived states occur for $Re > 300$, but if one takes poloidal rings with \mathbf{e}_y instead of \mathbf{e}_x they occur for $Re > 270$ already. This strong dependence on the nature of the initial states indicates that the stable manifold of the repeller are curled up in the high-dimensional phase space. As the Reynolds number increases so does the region explored until it eventually overlaps with the initial state.

To summarise, we have presented evidence for a fractal transition region to long lived turbulent states in plane Couette flow. These turbulent states are transient and belong to a repeller. The density of long life times increases with Reynolds number. This scenario might be relevant for other shear flows without linear instability and perhaps for some systems with a subcritical transition.

[1] S. Chandrasekhar. *Hydrodynamic and hydromagnetic stability*. (Oxford University Press, Oxford, 1961).

[2] P. G. Drazin, W. H. Reid. *Hydrodynamic stability*. (Cambridge University Press, Cambridge, 1981).

[3] A.G. Darbyshire, T. Mullin. *J. Fluid Mech.* **289**, 83–114 (1995).

[4] F. Daviaud, J. Hegseth, P. Bergé. *Phys. Rev. Lett.* **69**, 2511–2514 (1992).

[5] O. Dauchot, F. Daviaud. *Europhys. Lett.* **28**, 225–230 (1994).

[6] D. Coles. *J. Fluid Mech.* **21**, 385–425 (1965).

[7] V. A. Romanov. *Funkt. Anal. Appl.* **7**, 137 (1973).

[8] S.A. Orszag, L.C. Kells. *J. Fluid Mech.* **96**, 159–205 (1980).

[9] A.J. Acheson. *Elementary fluid mechanics*. (Oxford University Press, Oxford, 1990).

[10] J. Zang, D. Stassinopoulos, P. Alstroem, M.T. Levinsen. *Phys. Fluids* **5**, 1722–1726 (1994).

[11] D. Stassinopoulos, J. Zang, P. Alstroem, M.T. Levinsen. *Phys. Rev. E* **59**, 1189–1193 (1994).

[12] J.T. Stuart. *J. Fluid. Mech.* **9**, 353–370 (1960).

[13] J. Watson. *J. Fluid. Mech.* **9**, 371–389 (1960).

[14] A. Rauh, T. Zachrau, J. Zoller. *Physica D* **86**, 603–620 (1995).

[15] L. Boberg, U. Brosa. *Z. Naturforsch.* **43a**, 697–726 (1988).

[16] L.N. Trefethen, A. E. Trefethen, S. C. Reddy, T.A. Driscoll. *Science* **261**, 578–584 (1993).

[17] T. Gebhardt, S. Grossmann. *Phys. Rev. E* **50**, 3705–3711 (1994).

[18] B.F. Farrell, P.J. Ioannou. *Phys. Rev. Lett.* **72**, 1188–1191 (1994).

[19] J. P. Crutchfield und K. Kaneko. *Phys. Rev. Lett.* **60**, 2715–2718 (1988).

[20] U. Brosa. *J. Stat. Phys.* **55**, 1303–1312 (1989).

[21] A. Schmiegel, B. Eckhardt. *in preparation*, (1997).

[22] N. Tillmark, P. H. Alfredsson. *J. Fluid Mech.* **235**, 89–102 (1992).

[23] N. Tillmark. *Europhys. Lett.* **32**, 481–485 (1995).

[24] S. Malerud, K. J. Måløy, W. I. Goldburg. *Phys. Fluids* **7**, 1949–1955 (1995).

[25] S. C. Reddy, D. S. Hennigson. *J. Fluid. Mech.* **252**, 209–238 (1993).

[26] B. Eckhardt, H. Aref. *Phil. Trans. R. Soc. Lond. A* **326**, 655–696 (1988).

[27] B. Eckhardt. *Physica D* **33**, 89–98 (1988).

[28] E. Ott. *Chaos in dynamical systems*. (Cambridge University Press, Cambridge, 1993).

[29] U. Brosa. *Z. Naturforsch.* **41 a**, 1141–1153 (1986).

[30] B. Eckhardt, A. Mersmann, H. de Vries. *preprint*, (1997).

[31] M. Nagata. *J. Fluid Mech.*, **217**, 519–527, (1990).

[32] R.M. Clever, F.H. Busse. *J. Fluid Mech.* **234**, 511–527 (1992).

[33] R.M. Clever, F.H. Busse. In J. Grue et al., editors, *Waves and nonlinear processes in hydrodynamics*, 209–226. (Kluwer Academic Publishers, Amsterdam, 1996), and preprint (1997).